Appl Compos Mater (2013) 20:891–905
DOI 10.1007/s10443-012-9277-4

Notch Sensitivity of Fatigue Behavior of a Hi-Nicalon™/ SiC-B_4C Composite at 1,200 °C in Air and in Steam

M. B. Ruggles-Wrenn · G. Kurtz

Received: 7 May 2012 / Accepted: 21 June 2012 / Published online: 24 January 2013

Abstract The effect of holes on the fatigue life of a non-oxide ceramic composite processed via chemical vapor infiltration (CVI) was examined at 1,200 °C in laboratory air and in steam. The effect of holes on tensile strength at 1,200 °C was also evaluated. The composite comprised laminated woven Hi-Nicalon™ fibers in an oxidation inhibited matrix, which consisted of alternating layers of silicon carbide and boron carbide. Fiber preforms had pyrolytic carbon fiber coating with boron carbon overlay applied. Unnotched specimens and specimens with a center hole having a radius to width ratio of 0.24 were tested in tension-tension fatigue at 0.1 Hz and at 1.0 Hz. The fatigue stresses ranged from 100 to 140 MPa in air and in steam. Fatigue run-out was defined as 10^5 cycles at 0.1 Hz and as 2×10^5 cycles at 1.0 Hz. The net-section strength was less than the unnotched ultimate tensile strength. Comparison of notched and unnotched data also revealed that the fatigue performance was notch insensitive in both air and steam environments. Composite microstructure, as well as damage and failure mechanisms were investigated.

Keywords Ceramic-matrix composites (CMCs) · Fatigue · High-temperature properties · Mechanical properties · Fractography · Notch sensitivity

1 Introduction

Advanced aerospace applications such as turbine engine components, spacecraft reentry thermal protection systems, and hypersonic flight vehicles require structural materials that exhibit superior long-term mechanical properties and retained properties under high temperature, high pressure, and varying environmental factors, such as moisture. Because of their low density, high strength and fracture toughness at high

The views expressed are those of the authors and do not reflect the official policy or position of the United States Air Force, Department of Defense or the U. S. Government.

M. B. Ruggles-Wrenn (✉) · G. Kurtz
Department of Aeronautics and Astronautics, Air Force Institute of Technology, Wright-Patterson Air Force Base, OH 45433-7765, USA
e-mail: marina.ruggles-wrenn@afit.edu

temperatures SiC/SiC ceramic composites are being evaluated for aircraft engine hot-section components [1–4]. Many of these components contain holes, cutouts, and fasteners that introduce stress and strain concentrations in the surrounding regions. The SiC-based CMCs exhibit inelastic deformation behavior associated with matrix cracking and interface debonding, thus providing damage tolerance in the presence of notches and holes [5–15]. Additionally, in these applications the composites will be subjected to cyclic loadings at elevated temperatures in oxidizing environments. Therefore a thorough understanding of the effects of holes and notches on the fatigue performance of SiC/SiC composites in service environments is critical to design with and life prediction for these materials.

Because their constituents are intrinsically oxidation-prone, the most significant problem hindering SiC/SiC composites is oxidation embrittlement [16]. Typically the embrittlement occurs once oxygen enters through the matrix cracks and reacts with the fibers and the fiber coatings [17–19]. The degradation of fibers and fiber coatings is generally accelerated in the presence of moisture [20]. Composite degradation may be further accelerated by cyclic loading, where the reaction gases are expelled from matrix cracks during unloading and oxidizing atmosphere is drawn into the composite through the matrix cracks during reloading [16]. The issue of improving the oxidation resistance of the SiC/SiC composites has been addressed through the design of innovative multilayered interphases [21–23] and of self-healing multilayered matrices [21, 23–27]. The multilayered matrices contain phases that facilitate glass formation at high temperatures thus healing the cracks and preventing oxygen from diffusing further into the composite and reaching the oxidation-prone fibers.

Several recent studies investigated the high-temperature mechanical behavior of the SiC/Si-B-C composites with self-healing matrices. Carrere and Lamon [28] evaluated high-temperature fatigue behavior of a Nicalon™-reinforced CVI composite with a matrix consisting of alternating layers of SiC and SiBC. Crack healing, limited oxidation damage and fiber creep were observed at 1,200 °C. Reynaud et al. [29] investigated cyclic fatigue of a CVI 2.5D Hi-Nicalon™/SiBC composite at 600 °C and at 1,200 °C in air. At 600 °C the fatigue lifetime was controlled by slow crack growth in the fibers, while at 1,200 °C the fatigue lifetime was controlled by fiber creep. Darzens et al. [30] studied creep damage mechanisms of the CVI composites consisting of Nicalon™ fibers and SiC-based self-healing matrices. At or above 1,200 °C, the creep deformation of the CMCs was governed by creep of the fibers. Carrere and Lamon [31] examined creep behavior of a CVI Nicalon™/Si-B-C composite with a multilayered self-healing matrix at 1,200 °C. The creep rate of the composite was controlled by creep of the fibers and interfacial debonding. No significant creep induced matrix cracking was observed. Ruggles-Wrenn et al. [32] studied tension-tension fatigue of a CVI Hi-Nicalon™/SiC-B_4C composite at 1,200 °C in air and in steam. It was found that the fatigue performance of the composite was controlled by the creep resistance of the Hi-Nicalon™ fibers.

Several authors studied the effects of different types of notches in CMCs. Mackin et al. [8, 9] investigated stress concentration factors and stress redistribution in various edge-notched CMCs. Suo et al. [12] and He et al. [13] carried out a detailed theoretical analysis of inelastic deformation mechanisms that control the stress redistribution in the vicinity of notches. Mackin et al. [8] and Keith and Kedward [11] measured notched strength of SiC-fiber-reinforced CMCs, particularly for edge-notched specimens. Haque et al. [33] determined stress concentrations associated with a circular hole in SiC/SiNC composite. The degree of notch sensitivity in the

experimental studies [8, 9, 33] was found to depend on the size of the hole. McNulty et al. [16] examined the effects of holes and notches on the fatigue life of a Sylramic™/SiC composite at 815 °C. At this temperature fracture of the Sylramic™/SiC CMC occurred by an oxidative embrittlement mechanism. Therefore the damage tolerance and notch insensitivity normally associated with inelastic straining could not be exploited. The authors recommended that composite structures with holes and notches be designed extremely conservatively to ensure long life-times (> 100 h).

This study investigates the effect of circular holes on fatigue life at 1,200 °C of a CVI ceramic composite comprised of Hi-Nicalon™ fibers, pyrolytic carbon fiber coating with boron carbide overlay and a SiC-based oxidation inhibited matrix. The matrix consists of alternating layers of SiC and B_4C. The sensitivity of fatigue life to stress concentrations is examined in fatigue tests on specimens with circular holes as well as on unnotched specimens. Fatigue tests were conducted at 1,200 °C in air and in steam, at 0.1 Hz and at 1.0 Hz for fatigue stresses ranging from 100 to 140 MPa. Composite microstructure, damage and failure mechanisms are discussed.

2 Material and Experimental Arrangements

The test material was Hi-Nicalon™/SiC-B_4C (Hi-N/SiC-B_4C) ceramic composite manufactured by Hyper-Therm High-Temperature Composites, Inc. (Huntington Beach, CA). The CMC was reinforced with Hi-Nicalon™ fibers woven in an eight-harness satin weave, and was processed by CVI. The matrix consists of alternating layers of silicon carbide and boron carbide. Laminated fiber preforms were produced from eight plies of woven fabric in a 0°/90° layup symmetric about mid-plane with warp and fill plies alternated. Prior to infiltration, the preforms were coated with pyrolytic carbon fiber coating (~0.40 μm thick) with boron carbide overlay (~1.0 μm thick) to decrease bonding between fibers and matrix. The composite had a finished fiber volume of ~35.1 % and a density of ~2.59 g/cm^3. The overall microstructure of the CMC is shown in Fig. 1.

All tests were performed at 1,200 °C using the experimental set-up detailed elsewhere [32]. To assess the effects of stress concentrators on fatigue life, straight sided specimens of width $2W$=18 mm with a center hole of diameter $2a$=4.4 mm (a/W=0.24) were used in this study. The specimens were machined by diamond grinding and were sealed after machining. The same procedures were used for testing in air and in steam. Tensile tests were performed in displacement control with a constant rate of 0.05 mm/s. Tension-tension fatigue tests were performed in load control with a ratio of minimum to maximum stress R=0.05 at the frequencies of 0.1 and 1.0 Hz. Fatigue run-out was set to10^5 cycles at 0.1 Hz. At 1,200 °C the cycle count of 10^5 represents the number of loading cycles expected in aerospace applications. At 1.0 Hz the fatigue run-out was set to 2 x 10^5 because longer run-out time could be accommodated at that frequency. All specimens that achieved run-out were tested in tension to failure at 1,200 °C in air to determine the retained strength and stiffness. It should be noted that in all tests strains were measured using an extensometer with a 12.5-mm gage length (see Ruggles-Wrenn et al. [32] for extensometer information). Thus the strain values reported here are strains averaged over the gage length and not the local strain values around the hole. It is noteworthy that in all tests reported in this study the failure occurred within the gage section of the extensometer.

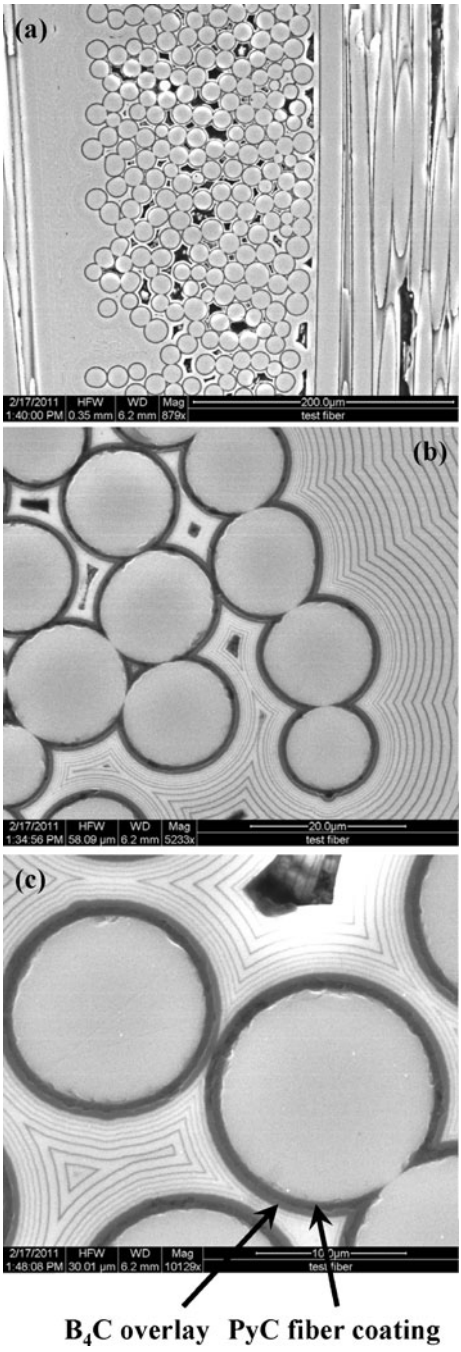

Fig. 1 SEM micrograph showing: **a** typical microstructure of the Hi-Nicalon™/SiC-B_4C ceramic composite, **b** self-healing matrix consisting of alternating layers of SiC and B_4C, **c** fibers and PyC fiber coating with B_4C overlay

3 Results and Discussion

3.1 Monotonic Tension

Tensile stress–strain behavior of the Hi-N/SiC-B_4C composite at 1,200 °C is typified in Fig. 2, where results for the unnotched specimens from prior work [32] are included for comparison. The stress–strain curve for notched specimen is based on the net-section area at the hole. The stress–strain curves for the notched as well as those for the unnotched specimens exhibit a nearly bilinear behavior. The stress–strain behavior is linear up to the proportional limit, where nonlinear behavior due to matrix cracking takes place. The presence of the center hole has no effect on this portion of the tensile stress–strain curve. Past the proportional limit, the stress–strain curves continue with a reduced slope. Furthermore, the change in slope is more pronounced in the case the unnotched specimens. The ultimate tensile strength (UTS) of the unnotched Hi-N/SiC-B_4C composite was 307 MPa, the elastic modulus was 208 GPa, and the failure strain was 0.69 %. The effect of hole on the net-section strength is evident. The strength decreased to 253 MPa, approximately 82 % of the unnotched strength at $2a$=4.4 mm. Similar reductions in strength due to the presence of the center hole (a/W=0.2) have been reported for Nicalon/SiC and Nicalon/MAS composites by McNulty et al. [7] and for Sylramic™/SiC composite by McNulty et al. [16].

3.2 Tension-Tension Fatigue

Results of the tension-tension fatigue tests are summarized in Table 1. Maximum net-section stress vs. time to failure (*S*-*T*) curves are presented in Fig. 3, where results for the unnotched specimens from prior work [32] are included for comparison.

Results in Fig. 3 reveal that the Hi-N/SiC-B_4C composite exhibits no notch sensitivity under cyclic loading at 1,200 °C in air. Essentially the same fatigue behavior was obtained with notched and unnotched specimens. For the notched as well as for the unnotched specimens, the fatigue run-out was achieved at 100 MPa, suggesting that the fatigue limit is between 100 and 120 MPa. Moreover, the same fatigue run-out stress of 100 MPa was produced at 0.1 Hz and at 1.0 Hz indicating that the fatigue frequency has little influence on the fatigue limit for both notched and unnotched specimens. Nevertheless, it should be noted that the fatigue limit at 0.1 Hz is based on a run-out condition of 10^5 cycles, while the fatigue

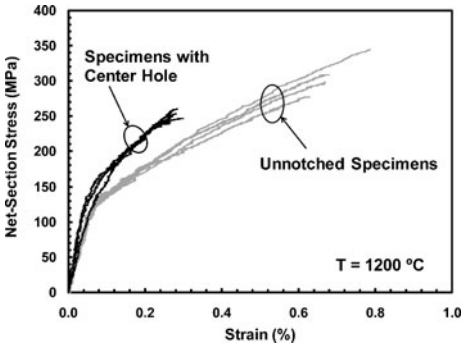

Fig. 2 Tensile stress–strain curves obtained for notched and unnotched Hi-Nicalon™/SiC-B_4C specimens at 1,200 °C in laboratory air. Data for unnotched Hi-Nicalon™/SiC-B_4C specimens from Ruggles-Wrenn et al. [32]

Table 1 Summary of fatigue results for Hi-Nicalon™/SiC-B_4C specimens with the center hole at 1,200 °C in laboratory air and in steam

Test Environment	Max Net-Section Stress (MPa)	Cycles to Failure	Time to Failure (h)
Fatigue at 0.1 Hz			
Laboratory Air	100	100,000[a]	278[a]
Laboratory Air	120	61,738	171
Laboratory Air	130	32,694	90.8
Laboratory Air	140	29,682	82.4
Steam	100	100,000[a]	278[a]
Steam	120	40,515	112
Steam	130	17,150	47.6
Steam	140	9,150	25.4
Fatigue at 1.0 Hz			
Laboratory Air	100	200,000[a]	55.6[a]
Laboratory Air	120	115,050	32.0
Laboratory Air	130	84,000	23.3
Laboratory Air	140	43,116	12.0
Steam	100	200,000[a]	55.6[a]
Steam	120	113,522	31.5
Steam	130	75,064	20.8
Steam	140	30,280	8.41

[a] Run-out, defined as 2×10^5 cycles at 1.0 Hz and as 10^5 cycles at 0.1 Hz. Failure of specimen did not occur when the test was terminated

limit at 1.0 Hz is based on a more demanding run-out condition of 2×10^5 cycles. Imposing a more rigorous run-out condition of 2×10^5 cycles at 0.1 Hz could result in a lower fatigue limit. Results in Table 1 also show some reductions in cyclic lifetimes produced at 0.1 Hz compared to those obtained at 1.0 Hz for peak net-section stresses above 100 MPa. For the peak net-section stress of 120 MPa the number of cycles to failure at 0.1 Hz was 61,738, a nearly 46 % reduction in cyclic life compared to that obtained at 1.0 Hz. For the peak net-section stresses of 130 and 140 MPa, the reductions in cyclic life due to drop in frequency by

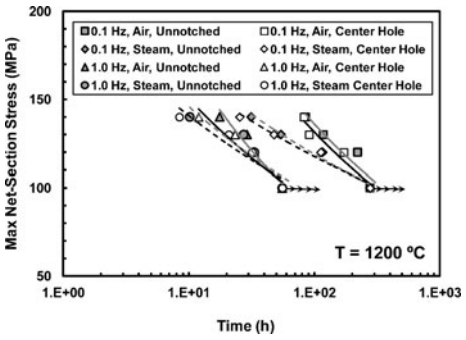

Fig. 3 Stress vs time to failure for notched and unnotched Hi-Nicalon™/SiC-B_4C specimens at 1,200 °C in air and in steam. Arrow indicates that failure of specimen did not occur when the test was terminated. Data for unnotched specimens from Ruggles-Wrenn et al. [32]

an order of magnitude were 61 % and 31 %, respectively. Contrastingly, the *S-T* curves in Fig. 3 demonstrate that for a given peak net-section stress, time to failure increases with decreasing frequency. It is noteworthy that similar reductions in cycles to failure and increases in times to failure due to decrease in fatigue frequency from 1.0 Hz to 0.1 Hz were observed for the unnotched specimens as well [32].

The fatigue performance of the Hi-N/SiC-B_4C composite remains notch insensitive in the presence of steam. At 1,200 °C in steam, fatigue performance of the notched specimens was largely the same as that of the unnotched specimens. Both notched and unnotched specimens achieved the fatigue run-out at the same stress level (100 MPa) in steam as in air. Furthermore, in steam the fatigue run-out stress remained independent of the fatigue frequency. All tests performed with the peak net-section stress of 100 MPa achieved run-out, regardless of the fatigue frequency or the test environment. At the loading frequency of 1.0 Hz for peak net-section stresses ≤120 MPa, the presence of steam continues to have little or no effect on the fatigue life. For σ_p=120 MPa, the time to failure in steam was approximately the same as that in air. For σ_p=130 MPa, the presence of steam reduced the time to failure by approximately 11 % for the notched specimens and by about 6 % for the unnotched specimens. For σ_p=140 MPa, the reduction in time to failure due to steam becomes a more significant 30 % for the notched specimens and 42 % for the unnotched specimens. However, at a lower fatigue frequency of 0.1 Hz the degrading effect of steam becomes considerable as soon as the peak net-section stress reaches 120 MPa. At 0.1 Hz, for the notched specimens the reduction in time to failure due to seam was 34 % for σ_p=120 MPa, 47 % for σ_p=130 MPa, and 69 % for σ_p=140 MPa. At 0.1 Hz, the reductions in time to failure due to steam for the unnotched specimens were similar (47 % for σ_p=120 MPa, 54 % for σ_p=130 MPa, and 63 % for σ_p=140 MPa).

Several notable features emerge from further consideration of the low cycle fatigue (LCF) behavior in Fig. 3. In the unnotched specimens, a fatigue limit was obtained at a stress level between 100 and 120 MPa, which corresponds closely to the matrix cracking stress $\sigma_{mc}\approx$ 100–120 MPa. Similar correlation between the fatigue limit and the matrix cracking stress has been reported previously for a CVI Sylramic™/SiC composite at 815 °C by McNulty et al. [16] and for a CVI Hi-Nicalon™/SiC composite at 1,200 °C by Ruggles-Wrenn et al. [34]. Note that the monotonic tension tests on the center-hole specimens yield the matrix cracking stress values similar to those obtained for the unnotched specimens (Fig. 2). Hence, it is hardly surprising that for the center-hole specimens, the fatigue limit is essentially the same as that for the unnotched specimens.

When the applied loads are above the matrix cracking stress, σ_{mc}, the LCF behavior of the CVI SiC/SiC composites at elevated temperature is governed by oxidation embrittlement. Under such loads, matrix cracks are formed during the first loading cycle. Oxygen enters the matrix cracks bridged by fibers causing severe oxidation and subsequent degradation of the fiber-matrix interphase. As a result the reaction products are formed that bond exposed fibers together. Load sharing by the fused fibers causes local stress concentrations that lead to fiber failures creating unbridged microcracks. Thus the oxidation-induced growth of matrix cracks becomes the life-limiting mechanism of the composite. McNulty et al. [16] pointed out that in center-hole specimens fracture also occurs by an oxidative embrittlement mechanism. However, in this case a fatigue limit is obtained at a lower stress $\approx \sigma_{mc}/k_c$, where k_c=2.5 is the elastic stress concentration factor. However, the oxidation embrittlement of the Hi-N/SiC-B_4C composite studied in this effort is limited by the self-healing matrix. When exposed to air and especially to steam at 1,200 °C, the multilayered SiC-B_4C matrix forms a fluid oxide phase that fills the matrix cracks as soon as they form under applied load. The glassy phases seal the matrix cracks and inhibit the oxygen from entering the composite through the cracks and attacking the

SiC fibers. Hence the oxidation resistance of the composite is increased [21]. McNulty et al. [16] observed regions of particularly severe oxidation near the hole edge in the center-hole specimens of CVI SiC/SiC composite tested in LCF at 815 °C. In contrast, the multilayered self-healing matrix of the Hi-N/SiC-B_4C composite effectively sealed both notched and unnotched specimens against further environmental ingress. Ruggles-Wrenn et al. [32] reported that the fatigue life of the unnotched Hi-N/SiC-B_4C composite at 1,200 °C in air and in steam was controlled mainly by the creep resistance of the fibers and, to a much smaller extent, by the oxidation embrittlement. Results in Fig. 3 suggest that the same mechanisms control the LCF of the notched Hi-N/SiC-B_4C specimens.

Evolution of the stress–strain hysteresis response with fatigue cycles of Hi-N/SiC-B_4C specimens with the center hole is typified in Fig. 4. In all tests, regardless of the test environment, the slope of the hysteresis loops decreases with increasing number of fatigue cycles, indicating progressive decrease in modulus. Moreover, it is seen that the strain ratcheting (progressive strain accumulation with cycles) takes place in all tests. The same observations were made for the center-hole specimens tested at 0.1 Hz. Significant increase in permanent strain with fatigue cycling at 1,200 °C was also reported by Reynaud et al. [29] for Hi-Nicalon™/SiBC and by Ruggles-Wrenn et al. [32] for unnotched Hi-N/SiC-B_4C. Reynaud and co-authors attributed this phenomenon mainly to creep of fibers. It is likely that creep of fibers is largely responsible for the strain ratcheting and modulus decrease seen in this study. However, these phenomena may be also caused by matrix cracking and formation of glass within the matrix cracks, which prevents closure of the cracks during unloading.

Cyclic strains vs fatigue cycles for tests performed at 1,200 °C in air and in steam are presented in Fig. 5 (a) and (b), respectively. Once more it is seen that strain ratcheting takes place in all tests. In the 1.0 Hz tests, ratcheting develops gradually, and becomes pronounced in the latter part of the tests. Contrastingly, decrease in fatigue frequency to 0.1 Hz causes an increase in strain accumulation rate and, thus, an earlier onset of strain ratcheting. Results in Fig. 5 (a) and (b) reveal that the largest strains are accumulated at 0.1 Hz in air. Strains accumulated at 0.1 Hz in steam are lower than those accumulated in air for the same maximum stress. The presence of steam appears to have little effect on strains accumulated in the 1.0 Hz tests performed with $\sigma_{max}<130$ MPa. However, for $\sigma_{max}\geq 130$ MPa, strains accumulated at 1.0 Hz in steam are lower than those accumulated at 1.0 Hz in air. Generally lower strain accumulation with fatigue cycling suggests that less microstructural damage has occurred, and that it is mainly limited to some additional matrix cracking. However, in the present study, lower strain accumulations in steam are consistent with the shorter fatigue lifetimes and are more likely caused by early bundle failures leading to specimen failure.

Another indication of damage development in fatigue is the change in the composite modulus (hysteresis modulus determined from the maximum and minimum stress–strain data points during a load cycle). The decrease in normalized modulus (i. e. modulus normalized by the modulus obtained on the first cycle) with fatigue cycles at 1,200 °C in air and in steam is shown in Fig. 6 (a) and (b), respectively. As expected, modulus loss increases with increasing fatigue stress. In tests performed at 1.0 Hz with $\sigma_{max}\leq 130$ MPa the presence of steam has relatively little effect on the modulus change with cycling (or on the fatigue lifetimes). Nevertheless, at 1.0 Hz and at σ_{max} of 140 MPa, modulus decay is accelerated due to steam. In contrast, the presence of steam has a noticeable effect on the modulus in tests conducted at 0.1 Hz. Modulus loss was considerably greater in tests performed at 0.1 Hz in steam than in those performed in air, suggesting an increase in the rate of microstructural damage development in steam. This result is consistent with the reduced fatigue lifetime produced at this frequency in steam. Note that at 0.1 Hz, the degrading effect of steam on modulus is noted for all fatigue stress levels above 100 MPa.

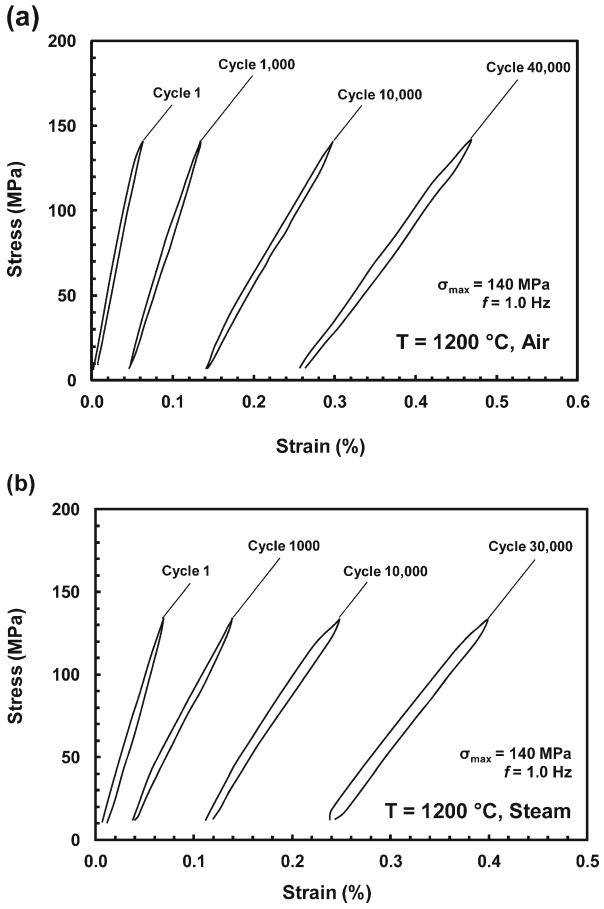

Fig. 4 Typical evolution of stress–strain hysteresis response with fatigue cycles of Hi-Nicalon™/SiC-B_4C specimens with the center hole at 1,200 °C: **a** in air, **b** in steam. Fatigue frequency is 1.0 Hz and maximum net section stress is 140 MPa

Similar modulus decrease with cycles was observed by Carrere and Lamon for Nicalon™/SiBC [28] and by Reynaud et al. for SiC/SiBC [29] CVI composites with self-healing matrices subjected to fatigue at 1,200 °C in air. Whereas the initial decrease in modulus is likely due to increase in matrix crack density [35], the continuing reduction in modulus is believed to be associated with glass formation in the matrix.

All specimens that reached run-out in fatigue tests were tested in tension to failure at 1,200 °C to measure the retained tensile strength. Such measurement of the retained tensile properties provides information about the extent of degradation due to prior fatigue loading, which is critical to the design community. Retained strength values of the center-hole specimens that achieved fatigue run-out are given in Table 2. All specimens subjected to prior fatigue suffered significant loss of tensile strength, regardless of the fatigue frequency. Test environment also had little effect on strength retention. Specimens subjected to 10^5 cycles at 0.1 Hz exhibited 24-26 % reduction in tensile strength, while the specimens subjected to 2×10^5 cycles at 1.0 Hz showed ~17 % reduction in strength. This considerable loss of

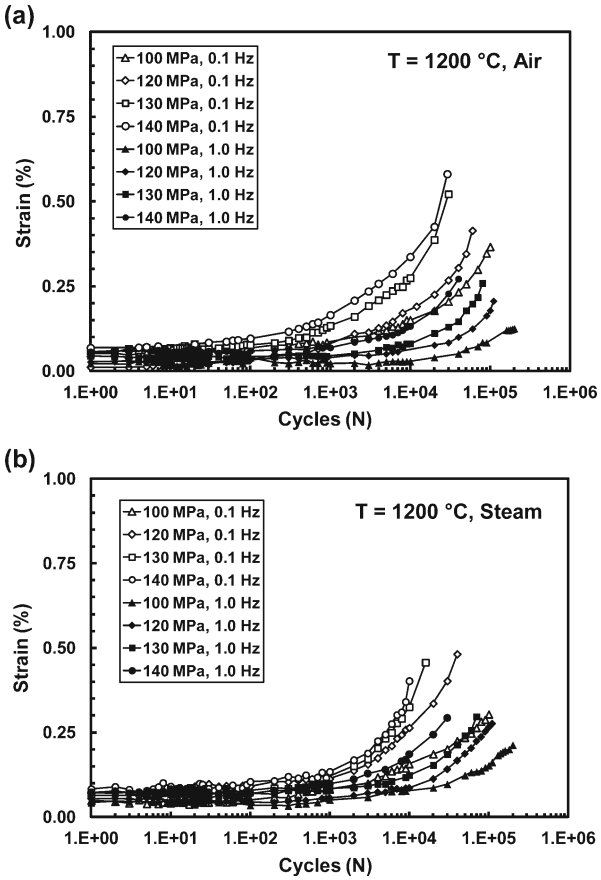

Fig. 5 Maximum strain vs. fatigue cycles for Hi-Nicalon™/SiC-B_4C specimens with the center hole at 1,200 °C: **a** in air and **b** in steam

tensile strength is believed to be caused by fiber degradation due to an intrinsic creep-controlled flaw growth mechanism [4]. Degradation of SiC fibers at elevated temperatures due to creep has been extensively studied and well documented; the cause of such degradation can be linked to atomic diffusional mechanisms [4, 36].

3.3 Composite Microstructure

After a specimen failed the testing system was promptly shut off and the bottom half of the failed specimen was removed from the furnace. Consequently the fracture surface of that half of the failed specimen was exposed to significant temperatures for a few minutes at most. These are the fracture surfaces that were examined with the SEM.

Fracture surface of the center-hole specimen tested in fatigue at 1.0 Hz with the maximum net section stress of 140 MPa at 1,200 °C in steam is presented in Fig. 7. This fracture surface is typical of the fracture surfaced obtained in this study. Notably the fracture surfaces produced in this effort do not exhibit large *oxidized* regions, which were observed in a previous study of Hi-Nicalon/SiC (Hi-N/SiC) composite tested in fatigue at 1,200 °C in air and in steam [34]. In the case of the Hi-N/SiC composite, a large portion of each fracture

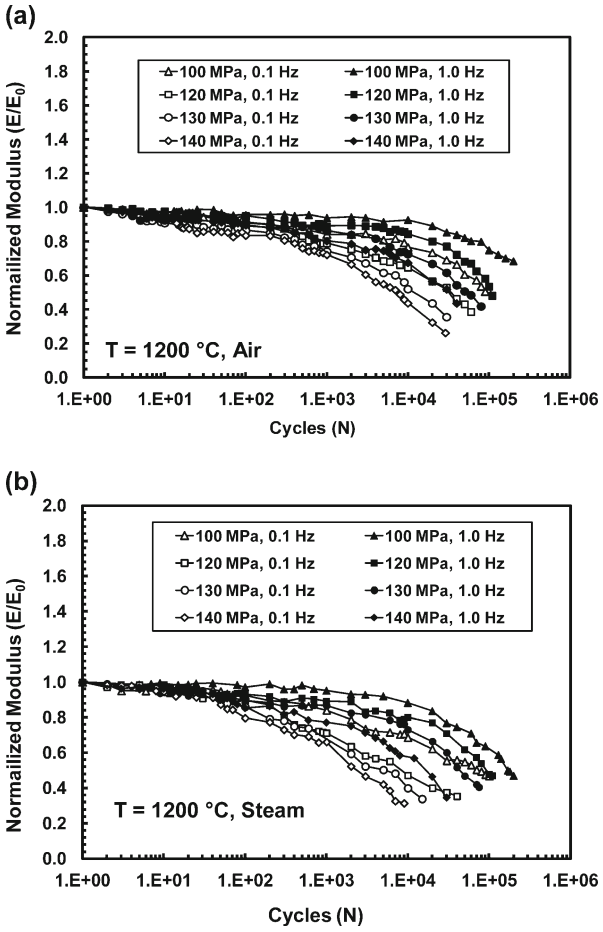

Fig. 6 Normalized modulus vs fatigue cycles for Hi-Nicalon™/SiC-B_4C specimens with the center hole at 1,200 °C: **a** in air and **b** in steam

surface was *oxidized*, pointing to an oxidation-assisted unbridged crack having grown before an ultimate failure of the composite [34]. As soon as the load is applied, the fiber-bridged matrix cracks form on the surface of the composite. Once these cracks are exposed to an

Table 2 Retained tensile strength of the Hi-Nicalon™/SiC-B_4C specimens with the center hole subjected to prior fatigue at 1,200 °C in laboratory air and in steam

Fatigue stress (MPa)	Fatigue environment	Retained strength (MPa)	Strength retention (%)
Prior fatigue at 0.1 Hz			
100	Air	192	76
100	Steam	187	74
Prior fatigue at 1.0 Hz			
100	Air	210	83
100	Steam	211	83

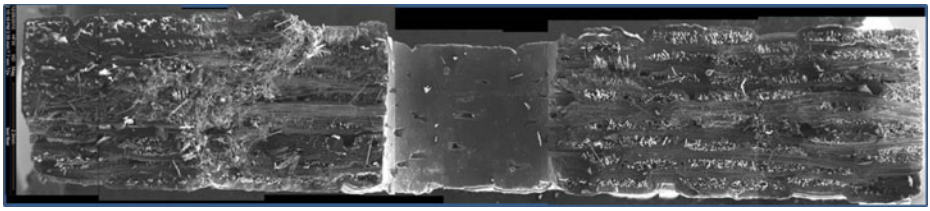

Fig. 7 Fracture surface of the center-hole specimen tested in fatigue at 1.0 Hz with maximum net section stress of 140 MPa at 1,200 °C in steam

oxidizing environment, oxygen enters the composite through the cracks and reacts with the BN fiber coating and SiC to form the reaction products, which fuse the fibers together [4, 34, 37]. After the fused fibers in the oxidized matrix cracks fail the unbridged cracks of substantial depth develop. Because of these unbridged matrix cracks the load is now redistributed to the intact interior region of the composite, ultimately leading to composite failure.

The distinguishing characteristic of the fracture surfaces produced in fatigue tests in the present study is that they are predominantly *not oxidized*. The size of the *oxidized* region, characterized by planar fracture as well as by oxidation of fibers and matrix, is negligible. The embrittlement is limited to a narrow band around the outside edge of the fracture surface. The rest of the fracture surface is *not oxidized*. This unembrittled region covers over ~90 % of the fracture surface, exhibits typical fiber pull-out and shows no visible signs of oxidation. Higher magnification images in Fig. 8 (a) and (b) show evidence of oxidation found in the *oxidized* region of the fracture surface in Fig. 7. Oxidation of fibers and matrix are apparent (8(a)) as is the glassy phase covering the fracture surface (Fig. 8(b)). Figure 8(c) depicts the transition from the *oxidized* region around the periphery to the *not oxidized* region in the interior of the fracture surface. Figure 8(d) shows an area of fiber pull-out, typical of the *not oxidized* region of the fracture surface.

These observations suggest that that oxidation embrittlement did not cause fatigue failure of the Hi-N/SiC-B_4C specimens with the center hole. Most likely the fiber-bridged matrix cracks form on the surface of the composite during the first loading cycle. Once the composite is exposed to the oxidizing environment at elevated temperature, oxygen diffuses through the crack network and reacts with the B_4C layers of the multilayered self-healing matrix to produce fluid oxide phases that fill the cracks as soon as they are initiated. Thus, the oxygen is trapped in the oxide phases as it continues to diffuse through the crack network and cannot attacking the oxidation-prone load-bearing fibers [21, 24–26]. Therefore oxidation embrittlement is observed only in a narrow band around the periphery of the fracture surface, while the rest of the fracture surface remains unembrittled. Damage and ultimate failure of the CMC in air and in steam are due to a fiber degradation mechanism not caused by oxidation.

High-temperature stress-rupture behavior of Hi-Nicalon fibers in air and in inert gas environment was studied extensively by Yun and DiCarlo [38–40] and DiCarlo et al. [41]. Based on experimental observations Yun, DiCarlo and co-workers concluded that the time-dependent fracture of the Hi-Nicalon fibers and of the Hi-Nicalon fiber-reinforced CMCs was controlled by creep-induced flaw growth in the fibers. The Hi-N/SiC-B_4C composite studied in this effort does not fail by oxidation embrittlement. The self-healing multilayered matrix appears to effectively seal the composite against further environmental ingress. Most likely creep of fibers is taking place. Fiber degradation is attributed to an intrinsic creep-controlled flaw growth mechanism. Thus it is believed that the fatigue lifetime of the Hi-N/SiC-B_4C

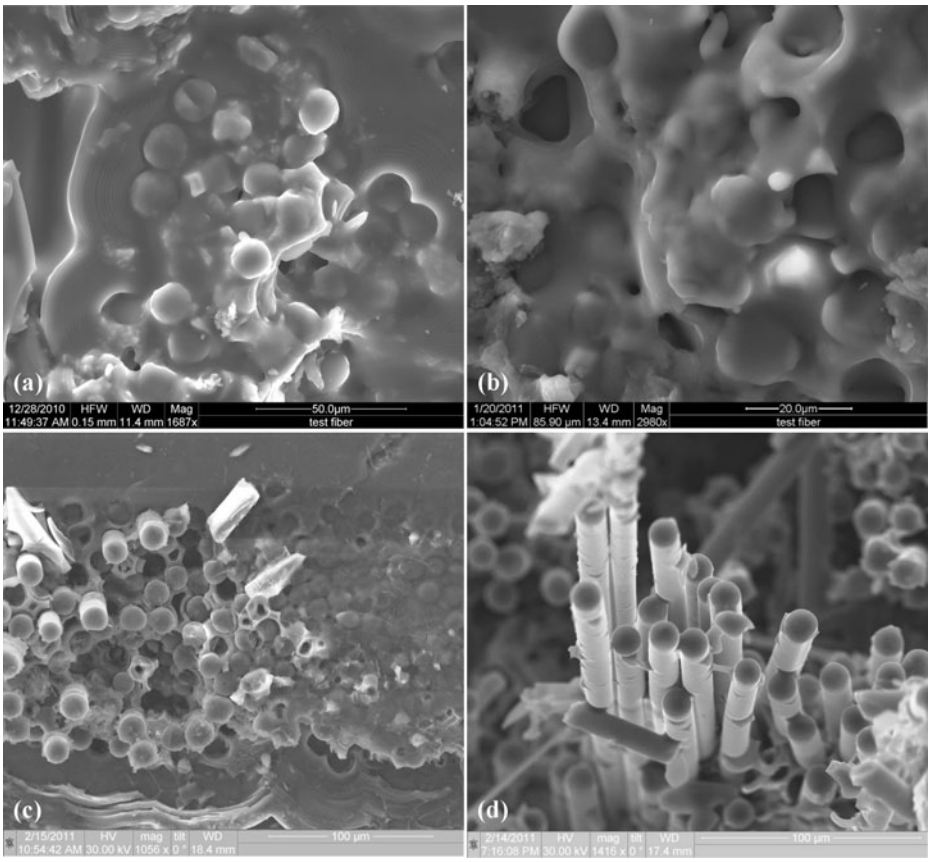

Fig. 8 Fracture surface of the center-hole specimen tested in fatigue at 1.0 Hz with maximum net section stress of 140 MPa at 1,200 °C in steam. Higher magnification images showing: **a** oxidation of fibers and matrix in the *oxidized* region, **b** glassy phase in the *oxidized* region, **c** *oxidized* region on the right transitioning to the *not oxidized* region on the left **d** fiber pull-out typical in the *not oxidized* region

composite is controlled to a large extent by the creep resistance of the Hi-Nicalon™ fibers. Furthermore, results presented here reveal that the presence of the center has no effect on the fatigue performance of the composite.

4 Concluding Remarks

The effect of center on tensile strength of the Hi-Nicalon™/SiC-B_4C composite was investigated at 1,200 °C. The net-section strength of the specimens with the center hole was approximately 82 % of the UTS of the unnotched specimens. The notch sensitivity of the tensile strength of the Hi-N/SiC-B_4C composite at 1,200 °C temperature is consistent with the results reported for other SiC/SiC CMCs. Typically ~25 % reduction in net-section strength is reported for center holes of 6-mm diameter [16]. This fairly small amount of notch sensitivity can be explained on the basis of the stress redistribution caused by local inelastic straining. The notch sensitivity appears to be diminished slightly at elevated temperature [16].

The tension-tension fatigue performance of the Hi-N/SiC-B_4C composite exhibits no notch sensitivity at 1,200 °C in air. The unnotched LCF fatigue limit for the Hi-N/SiC-B_4C composite at 1,200 °C is dictated by the matrix cracking stress ($\sigma_{mc} \approx 100–120$ MPa). The LCF fatigue limit for the center-hole specimens is similarly dictated by the matrix cracking stress, which in the case of the Hi-N/SiC-B_4C composite also is≈100–120 MPa. Thus it is hardly surprising that the fatigue run-out was achieved at 100 MPa for both notched and unnotched specimens. The fatigue frequency has no influence on notch sensitivity of the Hi-N/SiC-B_4C composite under cyclic loading at 1,200 °C in air. Furthermore, the fatigue performance of the composite remains notch insensitive at 1,200 °C in steam.

Prior fatigue caused significant diminution of tensile strength, indicating that damage occurred to the fibers. However, strength retention was notch insensitive. Reductions in tensile strength due to prior fatigue were not affected by the presence of the center hole. Presence of steam had negligible effect on strength retention.

The damage and failure of the Hi-N/SiC-B_4C composite at 1,200 °C in air and in steam are believed to be due to the creep of fibers. The oxidation embrittlement of the fibers is limited by the multilayered self-healing matrix, which reacts with oxygen and forms fluid oxide phases that seal the matrix cracks as soon as they are formed. The oxygen thus becomes trapped in the glassy phases and prevented from attacking the fibers. The fatigue performance of the Hi-N/SiC-B_4C composite is controlled mainly by the creep resistance of the fibers. The damage and failure mechanisms of the Hi-N/SiC-B_4C composite are notch insensitive.

References

1. Brewer, D.: HSR/EPM combustor materials development program. Mater. Sci. Eng. A **261**, 284–291 (1999)
2. Brewer, D., Ojard, G., Gibler, M.: Ceramic matrix composite combustor liner rig test. ASME Turbo Expo 2000, Munich Germany, May 8-11, 2000, ASME Paper 2000-GT-0670 (2000).
3. Corman, G.S., Luthra, K.: Silicon melt infiltrated ceramic composites (HiPerComp). In: Bansal, N. (ed.) Hand book of ceramic composites, pp. 99–115. Kluwer, NY (2005)
4. Morscher, G.N., Ojard, G., Miller, R., Gowayed, Y., Santhosh, U., Ahmad, J., John, R.: Tensile creep and fatigue of Sylramic-iBN melt-infiltrated SiC matrix composites: retained properties, damage development, and failure mechanisms. Comp. Sci. Tech. **68**, 3305–3313 (2008)
5. Droillard, C., Lamon, J.: Fracture toughness of 2D woven SiC/SiC CVI composites with multilayered interphases. J. Am. Ceram. Soc. **79**(4), 849–58 (1996)
6. Kagawa, Y., Goto, K.: Notch sensitivity of two-dimensional woven SiC fiber-reinforced SiC matrix composite fabricated by the polymer conversion process. J. Mater. Sci. Lett. **16**, 850–854 (1997)
7. McNulty, J.C., Zok, F.W., Genin, G., Evans, A.G.: Notch-sensitivity of fiber-reinforced ceramic-matrix composites: effects of inelastic straining and volume-dependent strength. J. Am. Ceram. Soc. **82**(5), 1217–1228 (1999)
8. Mackin, T.J., Purcell, T.E., Ming, Y.H., Evans, A.G.: Notch sensitivity and stress redistribution in three ceramic-matrix composites. J. Am. Ceram. Soc. **78**(7), 19–28 (1995)
9. Mackin, T. J., Purcell, T. E.: The use of thermoelasticity to evaluate stress redistribution and notch sensitivity in ceramicmatrix composites. Exp. Tech. 19–20 (1996)
10. Keith, W.P., Kedward, K.T.: Shear Damage Mechanisms in a Woven, Nicalon-Reinforced Ceramic-Matrix Composite. J. Am. Ceram. Soc. **80**(2), 357–64 (1997)
11. Keith, W.P., Kedward, K.T.: Notched strength of ceramic-matrix composites. Comp. Sci. Tech. **57**, 631–635 (1997)
12. Suo, Z., Ho, S., Gong, X.: Notch Ductile-to-Brittle transition due to localized inelastic band. J. Eng. Mater. Tech. **115**, 319–26 (1993)
13. He, M.Y., Wu, B., Suo, Z.: Notch-sensitivity and shear bands in brittle matrix composites. Acta Metall. Mater. **42**(9), 3065–70 (1994)
14. Gu, P.: Notch sensitivity of fiber-reinforced ceramics. Int. J. Fract. **70**(3), 253–266 (1994–1995)

15. Sunar, K.R.: Notch-sensitive fracture behavior of a silicon carbide fiber-reinforced glass-ceramic at elevated temperature. J. Mater. Eng. Perf. **7**(1), 104 (1998)
16. McNulty, J.C., He, M.Y., Zok, F.W.: Notch sensitivity of fatigue life in a Sylramic™/SiC composite at elevated temperature. Comp. Sci. Tech. **61**, 1331–38 (2001)
17. Prewo, K.M., Batt, J.A.: The oxidative stability of carbon fibre reinforced glass-matrix composites. J. Mater. Sci. **23**, 523–5271 (1988)
18. Mah, T., Hecht, N.L., McCullum, D.E., Hoenigman, J.R., Kim, H.M., Katz, A.P., Lipsitt, H.A.: Thermal stability of SiC fibres (Nicalon). J. Mater. Sci. **19**, 1191–1201 (1984)
19. Heredia, F.E., McNulty, J.C., Zok, F.W., Evans, A.G.: An oxidation embrittlement probe for ceramic matrix composites. J. Am. Ceram. Soc. **78**, 2097–100 (1995)
20. More, K.L., Tortorelli, P.F., Ferber, M.K., Keiser, J.R.: Observations of accelerated silicon carbide recession by oxidation at high water-vapor pressures. J. Am. Ceram. Soc. **83**(1), 211–213 (2000)
21. Naslain, R.: Design, preparation and properties of non-oxide CMCs for application in engines and nuclear reactors: an overview. Comp. Sci. Tech. **64**, 155–170 (2004)
22. Naslain, R., Pailler, R., Lamon, J.: Single- and multilayered interphases in SiC/SiC composites exposed to severe environmental conditions: an overview. Int. J. Appl. Ceram. Technol. **7**(3), 263–75 (2010)
23. Naslain, R.: SiC-matrix composites: nonbrittle ceramics for thermostructural applications. Int. J. Appl. Ceram. Technol. **2**(2), 75–84 (2005)
24. Lamouroux, F., Bertrand, S., Pailler, R., Naslain, R., Cataldi, M.: Oxidation-resistant carbon fiber reinforced ceramic-matrix composites. Comp. Sci. Tech. **59**, 1073–85 (1999)
25. Lamouroux, F., Bertrand, S., Pailler, R., Naslain, R.: A multilayer ceramic matrix for oxidation resistant carbon fibers-reinforced CMCs. Key. Eng. Matls. **164–165**, 365–8 (1999)
26. Darzens, S., Farizy, G., Vicens, J., Chermant, J.L.: Multiscale investigation of the creep behavior of SiCf-SiBC. In: Krenkel, W., et al. (eds.) High temperature ceramic matrix composites, pp. 211–217. Wiley-VCH, Weinheim (2001)
27. Quemard, L., Rebillat, F., Guette, A., Tawil, H., Louchet-Pouillerie, C.: Self-healing mechanisms of a SiC fiber reinforced multi-layered ceramic matrix composite in high pressure steam environments. J. Eur. Ceram. Soc. **27**, 2085–2094 (2007)
28. Carrere, P., Lamon, J.: Fatigue behavior at high temperature in air of a 2D woven SiC/SiBC with a self healing matrix. Key. Eng. Matls. **164–165**, 321–4 (1999)
29. Reynaud, P., Rouby, D., Fantozzi, G.: Cyclic fatigue behavior at high temperature of a self-healing ceramic matrix composite. Ann. Chim. Sci. Mat. **30**(6), 649–58 (2005)
30. Darzens, S., Chermant, J.L., Vicens, J., Sangleboeuf, J.C.: Understanding of the creep behavior of SiC_f–SiBC composites. Scripta Mat. **47**, 433–439 (2002)
31. Carrere, P., Lamon, J.: Creep behavior of a SiC/Si-B-C composite with a self healing matrix. J. Eur. Ceram. Soc. **23**, 1105–1114 (2003)
32. Ruggles-Wrenn, M.B., Delapasse, J., Chamberlain, A.L., Lane, J.E., Cook, T.S.: Fatigue behavior of a Hi-Nicalon™/SiC-B_4C composite at 1200°C in air and in steam. Mater. Sci. Eng. A **534**, 119–128 (2012)
33. Haque, A., Ahmed, L., Ramasetty, A.: Stress concentrations and notch sensitivity in woven ceramic matrix composites containing a circular hole—an experimental, analytical, and finite element study. J. Am. Ceram. Soc. **88**(8), 2195–2201 (2005)
34. Ruggles-Wrenn, M.B., Christensen, D.T., Chamberlain, A.L., Lane, J.E., Cook, T.S.: Effect of frequency and environment on fatigue behavior of a CVI SiC/SiC ceramic matrix composite at 1200 °C. Comp. Sci. Tech. **71**(2), 190–196 (2011)
35. Shuler, S.F., Holmes, J.W., Wu, X., Roach, D.: Influence of loading frequency on the room-temperature fatigue of a carbon-fiber/SiC-matrix composite. J. Am. Ceram. Soc **76**(9), 2327–36 (1993)
36. Yun, H.M., DiCarlo, J.A.: Time/temperature dependent tensile strength of SiC and Al_2O_3-based fibers. In: Bansal, N.P., Singh, J.P. (eds.) Ceramic Transactions, Advances in Ceramic-Matrix Composites III, 74, pp. 17–26. American Ceramic Society; p, Westerville OH (1996)
37. Morscher, G.N., Hurst, J., Brewer, D.: Intermediate-temperature stress rupture of a woven Hi-Nicalon, BN-interphase. SiC-matrix composite in air. J. Am. Ceram. Soc. **83**(6), 1441–9 (2000)
38. Yun, H.M., DiCarlo, J.A.: *Thermomechanical behavior of advanced SiC fiber multifilament tows*. NASA Technical Memorandum 107366. NASA Lewis Research Center. Cleveland OH (1996)
39. Yun, H.M., DiCarlo, J.A.: *Thermomechanical characterization of SiC fiber tows and implications for CMC*. NASA/TM-(1999)-209283. NASA Glenn Research Center. Cleveland OH (1999).
40. Yun, H.M., DiCarlo, J.A.: *Comparison of the tensile, creep, and rupture strength properties of stoichiometric SiC fibers*. NASA/TM-(1999)-209284. NASA Glenn Research Center. Cleveland OH (1999).
41. DiCarlo, J.A., Yun, H.M., Hurst, J.B.: Fracture mechanisms for SiC fibers and SiC/SiC composites under stress-rupture conditions at high temperatures. Appl. Math. Comp. **152**, 473–481 (2004)